4ICEGE Thessaloniki-GREECE 2007

4th International Conference on
Earthquake Geotechnical Engineering
June 25-28, 2007
Paper No. 1737

VARIATIONS OF SHEAR WAVE VELOCITY AT HUALIEN LSST SITE WITH RESPECT TO MAGNITUDE OF EARTHQUAKE SHAKINGS

Cheng-Hsing CHEN [1], Shang-Yi HSU[2]

ABSTRACT

This paper is to deduce the predominant frequency of ground vibration at the Hualien site by using the earthquake responses recorded. 22 events with peak ground acceleration distributed from a few gals to 142 gals were selected for analysis. Method of phase spectrum identification was used to identify the predominant frequencies of transfer function between the downhole earthquake response and the ground surface response. Based on that, the shear wave velocities of soil layer are deduced. Results show that both the predominant frequency of transfer functions calculated and the shear wave velocity of soil layers identified will decrease with respect to the magnitude of ground shaking. It can also be clearly identified that the Hualien site has anisotropic property in two horizontal directions.

Keywords: Shear wave velocity, earthquake ground motion, vertical array, predominant frequency.

INTRODUCTION

The behavior of soil nonlinearity plays an important role on the earthquake responses of ground as well as the supported structures. From the results of laboratory tests, it is well known that the shear modulus of soil will decrease significantly when it is subjected to larger cyclic shear strains (Seed and Idress, 1970). During earthquakes, some observations had found that the effects of soil nonlinearity will affect the amplification of ground responses (Wen, 1980). However, the effects of soil nonlinearity on the predominat frequency of ground vibration during earthquakes are seldom discussed.

The aim of this paper is to identify the predominant frequency of ground vibration during earthquakes by using the earthquake responses recorded at the site of Hualien Large Scale Seimic Test program. Furthermore, the shear wave velocities of soil layers at the Hualien site will also be deduced based on the predominant frequencies identified.

HUALIEN LARGE SCALE SEISMIC TEST

A Large Scale Seismic Test (LSST) had been carried out at Hualien, Taiwan, to investigate the effects of soil-structure interaction during dynamic loadings. It is an in-situ test program sponsored by EPRI and NRC of USA, CEA and EdF of France, TEPCO and CRIEPI of Japan, KINS and KEPCO of Korea and TPC of Taiwan (Tang, 1991). A quarter scale nuclear power plant containment model of diameter 10.82m and height 16.13m, as shown in Figure 1, was built on gravelly deposits for dynamic tests. Two phases of forced vibration tests had been conducted and large amount of earthquake responses had already been recorded.

[1] Professor, Department of Civil Engineering, National Taiwan University, Taiwan, Email: chchen2@ntu.edu.tw
[2] Associate Research Fellow, National Center for Research on Earthquake Engineering, Taiwan.

Figure 1. The 1/4 containment model at Hualien LSST

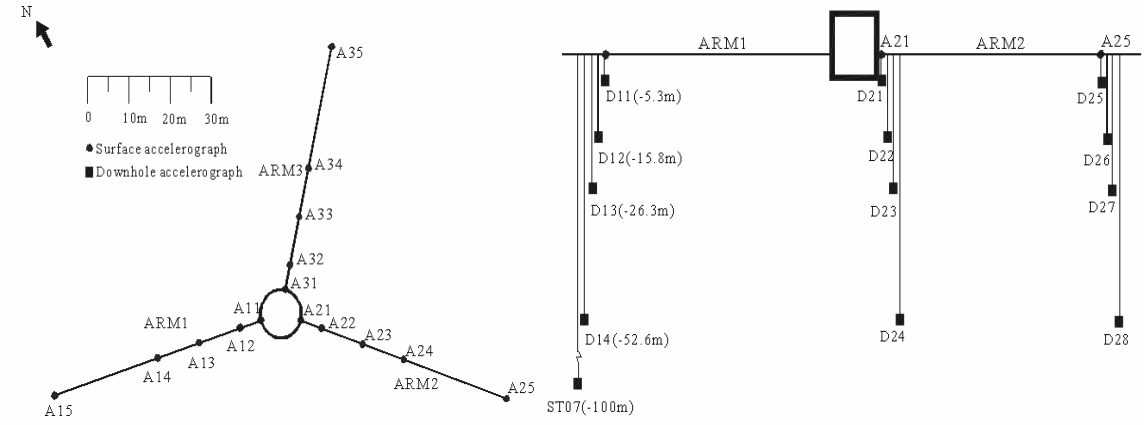

(a) Surface array (b) Downhole array

Figure 2. Layout of strong motion arrays at Hualien LSST

Layout of strong motion arrays

In Hualien Project, an intense strong motion array had been installed around the model structure, as shown in Figure 2. There are three surface linear arrays (designated as ARM1, ARM2 and ARM3, respectively), and three vertical arrays located under the stations A15, A25 and A21 (designated as A15, A25 and A21 vertical arrays, respectively). In each vertical array, four downhole accelerometers were installed at the depths of 5.3 m, 15.8 m, 26.3 m and 52.6 m, respectively. Since A15 and A25 vertical arrays are located at a distance of 52.6 m from the center of the containment model, they can be regarded as free-field arrays. In subsequent analyses, the motions recorded at the A15 vertical array will be adopted for ground motion analysis.

Strong ground motions selected

Since the completion of the LSST arrays at Hualien, a total of 113 earthquakes with local magnitude larger than 4 had been recorded in the period 1993 to 2002. Among them, 22 events will be selected for this study. They are listed as shown in Table 1. Those earthquakes have local magnitudes distributed from 4.6 to 7.3, including the disastrous Chi-Chi earthquake occurred on Sept. 20, 1999 (Event 9). The peak ground accelerations recorded at the surface station A15 are also shown in Table 1. They are distributed from a few gals to 142 gals.

Geological profile at the Hualien LSST site

The Hualien LSST site is located on thick gravelly deposits, namely the Meilung gravel formation. The geological profile near the ground surface is shown in Figure 3 (CRIEPI, 1993). The top 5 meters are loosely deposited sands. Below that, the gravel formation is massive unconsolidated conglomerate composed of pebbles varying in diameter from 10cm to 20cm. The distribution of shear wave velocities obtained from geophysical surveys (P-S logging) is also shown in Figure 3. The velocities increase from 133 m/s at the ground surface to about 550m/s at a depth of 50m.

Table 1. Earthquake data selected for analysis

EQ No.	ORIGIN TIME (UT)	LOCATION		LOCAL MAG. (ML)	PGA at A15 (gal.)		
		Lon. (E)	Lat. (N)		V	EW	NS
1	1994 01 20 05:50:17	121 51.83	24 03.53	5.6	24.52	43.77	32.12
2	1994 06 05 01:09:27	121 51.24	24 27.36	6.2	28.33	27.82	41.39
3	1994 10 05 01:13:38	121 43.13	23 09.22	5.8	12.03	38.76	27.39
4	1995 02 23 05:18:54	121 41.13	24 12.13	5.8	30.05	39.27	48.82
5	1995 05 01 14:50:45	121 31.99	24 02.66	4.9	115.48	73.73	135.79
6	1995 05 02 06:17:21	121 38.04	24 00.74	4.6	118.26	64.92	87.11
7	1995 10 07 11:08:37	121 40.34	23 51.58	4.7	4.76	10.05	7.34
8	1996 05 28 21:53:13	121 34.58	24 03.12	5	86.30	51.49	80.63
9	1999 09 20 17:47:15	120 48.93	23 51.15	7.3	31.89	86.03	73.92
10	1999 09 20 18:11:52	121 03.37	23 51.05	6.7	23.86	31.75	59.52
11	1999 09 20 18:16:16	121 02.19	23 50.39	6.7	10.08	30.42	30.50
12	1999 09 20 20:43:48	121 19.48	23 45.58	6.5	8.36	13.41	16.59
13	1999 09 21 00:23:07	—	—	—	22.04	7.31	15.03
14	1999 09 22 00:14:39	121 02.56	23 50.17	6.8	15.06	33.72	47.87
15	1999 10 16 12:31:55	121 19.42	24 00.13	5	6.90	15.77	16.61
16	1999 10 22 03:10:43	120 25.50	23 31.58	6	2.60	5.91	5.23
17	1999 11 01 17:53:02	121 45.33	23 21.71	6.9	29.01	29.01	59.32
18	2000 05 06 13:41:57	121 30.00	24 02.40	5.0	106.00	47.88	71.73
19	2000 07 14 00:07:32	121 43.70	24 02.90	5.7	21.04	141.96	74.01
20	2000 09 10 08:54:46	121 35.03	24 05.12	6.2	99.77	56.94	103.96
21	2000 10 24 07:11:47	121 31.47	23 54.12	4.8	35.58	49.86	57.85
22	2002 03 31 06:52:57	122 11.29	24 08.23	6.8	16.28	54.27	44.50

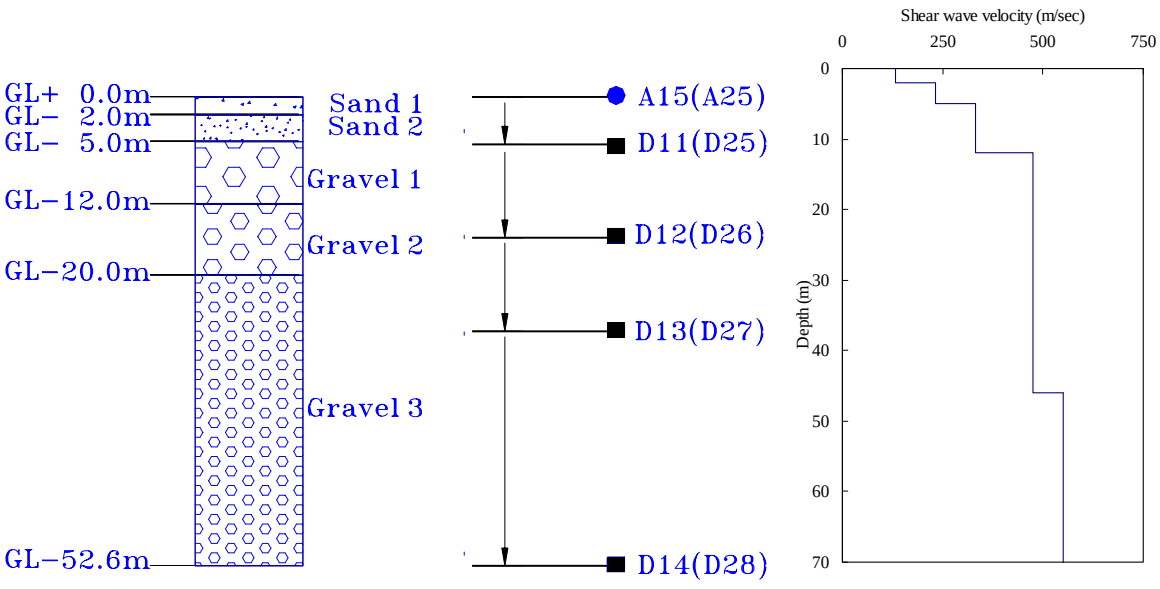

Figure 3. Geological profile at Hualien LSST site

SPECTRAL ANALYSIS

To investigate the characteristics of ground vibration, the earthquake data recorded from vertical arrays are very useful. The transfer function between the motions recorded at two depths can be used to identify the modal frequencies of vibration of soil layers through spectral analysis.

Transfer functions

Let the accelerogram recorded at certain depth be the *i*-series and the one on the ground surface be the 1-series. Through the applications of Fourier transforms, one can calculate the spectral ratio by

$$H_{i1}(f) = \frac{H_{ii}(f)}{H_{11}(f)} \tag{1}$$

where $H_{ii}(f)$ and $H_{11}(f)$ are the Fourier transforms of the i- and 1-series, respectively, and $H_{i1}(f)$ is the transfer function between i- and 1-series. The transfer function $H_{i1}(f)$ is a complex-valued function of frequency. Its absolute value defines the amplitude spectrum, and the arctangent value of the ratio between the imaginary and the real parts defines the phase spectrum. Both of them can be used to identify the modal frequencies of vibration for the soils in between. Usually, the amplitude spectrum is used to identify the modal frequencies. From the first valley of the amplitude spectrum, the predominant frequency can be determined. Furthermore, the predominant frequency can also be identified from the phase spectrum where the phase angle is equal to 90^0.

Phase spectrum identification

Theoretically, both the amplitude and phase spectra are continuous smooth function of frequency *f*. However, the real spectral ratios calculated from earthquake records are highly oscillated in general. In engineering applications, a lot of smoothing techniques have been proposed to smooth the amplitude function in order to identify where the predominant frequency is located. However, the amplitude function smoothed by averaging procedure is still wide-banded at most times and can not easily be used to determine the predominant frequency

.

In this paper, the technique of using phase spectrum to identify the lowest modal frequency will be used as an alternative method. The advantage of using this method is that the curve fitted to the phase spectrum will across the line of 90^0 with a very step slope so that the results of identification is not so sensitive to the method of curve fitting as in the case of using amplitude function. This method has been used by Chen and Chiu(1998). To illustrate the method of predominant frequency identification used in this study, the spectral analysis for the motions of A15 vertical array recorded in the Sept. 20, 1999 earthquake (Event 9) is shown below. Figures 4(a)~(d) are the phase spectra of the transfer functions of D11NS/A15NS, D12NS/A15NS, D13N8/A15NS and D14NS/A15NS, respectively. The frequency interval in those figures is very small ($\triangle f$=0.0061Hz) so that the data points look rather scattered. However, they are distributed like a monotonic increasing function starting from about 0^0 towards 360^0. Then, a polynomial of order 9 is used for curve fitting. From the fitted curve as shown in each figure, the frequency where the fitted curve across the line of 90^0 is the predominant frequency of associated soil layers. They are located at frequencies of 8.50Hz, 4.98Hz, 3.45Hz and 2.22 Hz, respectively.

Predominant frequencies

By using the same procedure, the predominant frequencies for all the earthquakes studies are identified as shown in Table 2. In each case, the frequency obtained can be recognized as the predominant frequency of soil layers between the ground surface and the depth when the designated downhole accelerometer located. Therefore, the thicker the soils are, the lower the modal frequency can be identified. It can also be observed from the results obtained, for the same earthquake, the predominant frequencies identified have lower values in the EW direction as compared to the results in the NS direction.

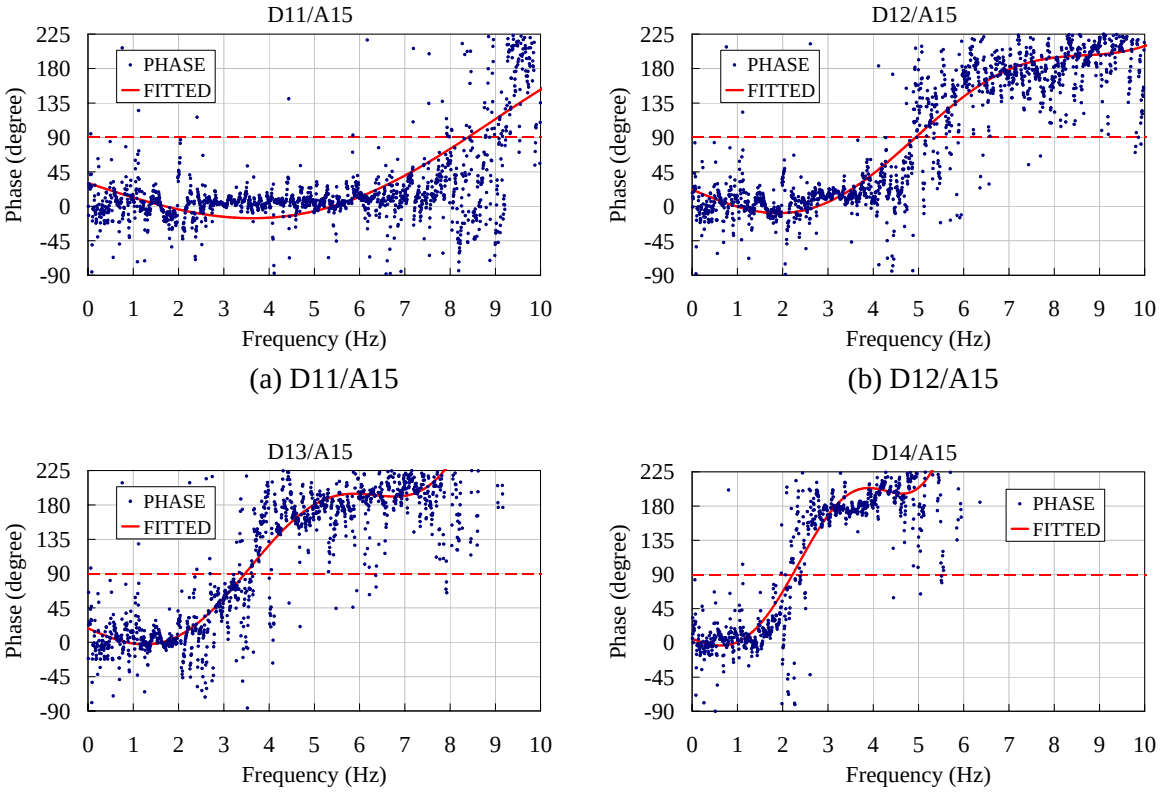

(a) D11/A15 (b) D12/A15

(c) D13/A15 (d) D14/A15

Figure 4. Phase spectrum of transfer functions-NS component

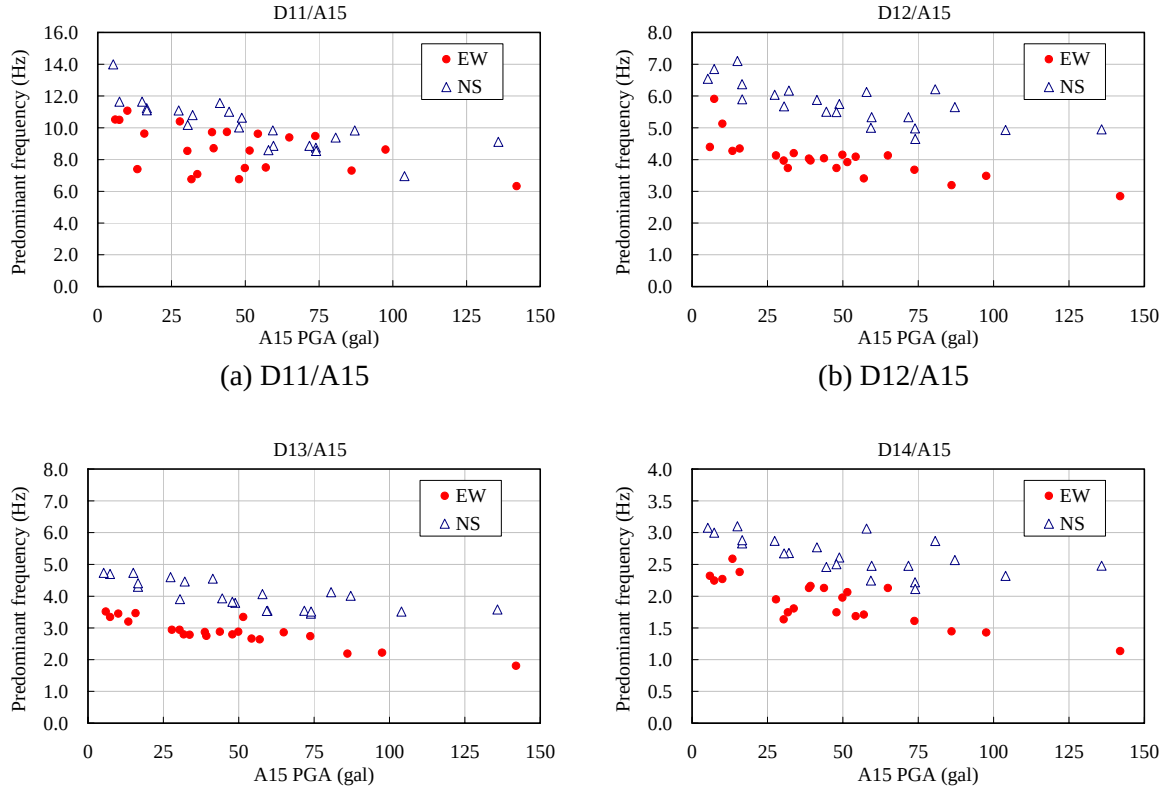

(a) D11/A15 (b) D12/A15

(c) D13/A15 (d) D14/A15

Figure 5. Predominant frequency of transfer functions vs. PGA at A15

Table 2. Predominant frequencies identified from transfer functions

EQ No.			1	2	3	4	5	6	7	8	9	10	11
	A15 PGA (gal.)		43.77	27.82	38.76	39.27	73.73	64.92	10.05	51.49	86.03	31.75	30.42
EW	D11/A15	f_{21}	9.74	10.40	9.72	8.71	9.48	9.39	11.08	8.57	7.30	6.76	8.54
	D12/A15	f_{31}	4.04	4.13	4.03	3.97	3.68	4.13	5.13	3.92	3.19	3.74	3.97
	D13/A15	f_{41}	2.88	2.94	2.87	2.75	2.74	2.86	3.45	3.34	2.19	2.80	2.94
	D14/A15	f_{51}	2.13	1.95	2.13	2.16	1.61	2.13	2.27	2.06	1.45	1.75	1.64
	A15 PGA (gal.)		32.12	41.39	27.39	48.82	135.79	87.11	7.34	80.63	73.92	59.52	30.50
NS	D11/A15	f_{21}	10.80	11.56	11.09	10.63	9.12	9.83	11.65	9.39	8.50	8.86	10.18
	D12/A15	f_{31}	6.17	5.88	6.04	5.75	4.95	5.65	6.85	6.21	4.98	5.33	5.68
	D13/A15	f_{41}	4.46	4.55	4.60	3.79	3.58	4.01	4.70	4.13	3.45	3.54	3.91
	D14/A15	f_{51}	2.68	2.77	2.87	2.61	2.48	2.57	3.00	2.87	2.22	2.48	2.67

EQ No.			12	13	14	15	16	17	18	19	20	21	22
	A15 PGA (gal.)		13.41	7.31	33.72	15.77	5.91	29.01	47.88	141.96	56.94	49.86	54.27
EW	D11/A15	f_{21}	7.40	10.50	7.08	9.63	10.52	8.63	6.76	6.32	7.50	7.47	9.62
	D12/A15	f_{31}	4.27	5.91	4.20	4.35	4.39	3.49	3.74	2.84	3.41	4.15	4.09
	D13/A15	f_{41}	3.20	3.34	2.78	3.47	3.52	2.22	2.80	1.81	2.64	2.88	2.66
	D14/A15	f_{51}	2.59	2.25	1.81	2.38	2.32	1.43	1.75	1.14	1.71	1.98	1.68
	A15 PGA (gal.)		16.59	15.03	47.87	16.61	5.23	59.32	71.73	74.01	103.96	57.85	44.50
NS	D11/A15	f_{21}	11.23	11.65	10.02	11.10	13.99	9.84	8.86	8.54	6.96	8.59	11.01
	D12/A15	f_{31}	6.37	7.10	5.49	5.90	6.54	5.00	5.33	4.65	4.93	6.13	5.51
	D13/A15	f_{41}	4.30	4.74	3.82	4.41	4.74	3.53	3.54	3.52	3.52	4.06	3.93
	D14/A15	f_{51}	2.83	3.10	2.50	2.88	3.08	2.25	2.48	2.11	2.32	3.06	2.46

Predominant frequency vs. PGA at A15

The earthquake events selected for analysis have different magnitude of ground shaking. The peak ground accelerations recorded at the surface station A15 are distributed from a few gals to 142 gals. When the predominant frequencies obtained are plotted with respect to the PGA recorded at A15 as shown in Figures 5(a)~(d), it can be clearly seen that the predominant frequency of vibration will decrease with the value of PGA at A15, i.e., with the magnitude of ground shaking. This is due to the effects of nonlinearity of soil when it is subjected to larger shear strains. It can also be observed from those figures, the predominant frequencies identified have lower values in the EW direction as compared to the results in the NS direction. It may be attributed from the effects of soil an-isotropic. The same results had been observed from the results of Forced vibrations performed on the containment of Hualien site (TEPCO, 1993; de Barros, 1995).

IDENTIFICATION FOR SHEAR WAVE VELOCITY

Four layer ground model

In A15 vertical array, the downhole accelerometers are located at depths of 5.3 m, 15.8 m, 26.3 m and 52.6 m, respectively. From the results of geological explorations as shown in Figure 3, it is known that the LSST site has a quite simple geological profile, a sand layer of thickness 5 m overlying a very thick gravel formation. The shear wave velocities shown in this figure are the results measured from the geophysical survey (PS-logging). They are usually regarded as the small strain velocity. Based on that, it is reasonable to adopt a simple ground model, as shown in Figure 6, for wave velocity identification. From ground surface to the depth of 52.6 m, the ground is divided into 4 layers according to the depths of downhole accelerometers. Each layer has thickness h_i and mass density ρ_i. The underlying soils are regarded as a half-space.

The ground motions excited by earthquakes are rather complex in nature. However, for engineering applications, it is often assumed that the horizontal ground motions are mainly produced by vertically propagating SH waves, i.e., the 1-D shear beam model can be applied. By substituting the predominant frequencies identified previously into the characteristic equations of SH wave traveling in the associated soil layers, the shear wave velocity of each layer can then be identified subsequently. It is noted that the damping ratio of soil has very little effect on the modal frequency of ground. Therefore, it is convenient to assume that the damping ratios of soils are all equal to zero in deriving the characteristic equation of soil layers. This leads to a real-valued characteristic equation which is much easier for calculation purpose.

Based on the theory of wave propagation, the characteristic equation of transfer function between different soil layer can be derived as follows.

Single Layer Over a Half-Space

For a single layer on top of an elastic half-space as shown in Figure 7(a), the transfer function can be written as

$$\frac{U_2}{U_1} = \cos\left(\frac{2\pi f h_1}{C_{s1}}\right) \tag{2}$$

Let f_{21} be the predominant frequency as identified from the transfer function between the first downhole station and the surface station, then the equivalent shear wave velocity for the first layer can be estimated by

$$C_{s1} = 4 f_{21} h_1 \tag{3}$$

Two Layer Over a Half-Space

For a system of two layers of soil on top of an elastic half-space as shown in Figure 7(b), the transfer function can be written as

$$\frac{U_3}{U_1} = \rho_2 C_{s2} \cos\left(\frac{2\pi f h_1}{C_{s1}}\right)\cos\left(\frac{2\pi f h_2}{C_{s2}}\right) - \rho_1 C_{s1} \sin\left(\frac{2\pi f h_1}{C_{s1}}\right)\sin\left(\frac{2\pi f h_2}{C_{s2}}\right) \tag{4}$$

The characteristic equation corresponding to the predominant frequency f_{31} is

$$\tan\left(\frac{2\pi f_{31} h_1}{C_{s1}}\right)\tan\left(\frac{2\pi f_{31} h_2}{C_{s2}}\right) = \frac{\rho_2 C_{s2}}{\rho_1 C_{s1}} \tag{5}$$

Given f_{31} from Table 2 and C_{s1} from previous model, C_{s2} is the first positive root of Eq.(5).

Multi-Layer System

For the system of 3 soil layers on top of an elastic half-space as shown in Figure 7(c), the upper two layers can be regarded as an equivalent uniform single layer of thickness $\overline{h}_1$ and velocity $\overline{C}_{s1}$ where

$$\overline{h}_1 = h_1 + h_2 \tag{6}$$

$$\overline{C}_{s1} = 4\overline{h}_1 \ f_{13.} \tag{7}$$

Now regard the upper three layers of soil as two layers of soil with thicknesses $\overline{h}_1$ and h_3 and shear wave velocities $\overline{C}_{s1}$ and C_{s3}, respectively, as shown in Figure 7(d). Then C_{s3} can now be solved based on Eq.(5) when the predominant frequency f_{41} is given from Table 2. For a system having more layers of soil, the same procedure can be used recursively to calculate the shear wave velocity for each layer.

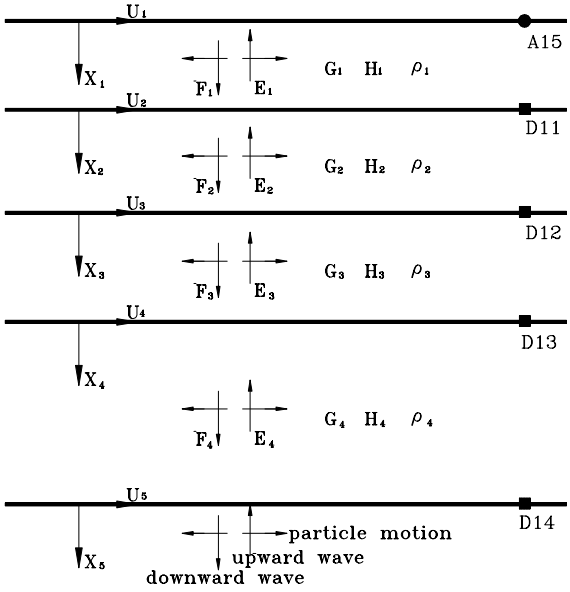

Figure 6. Ground model used for system identification

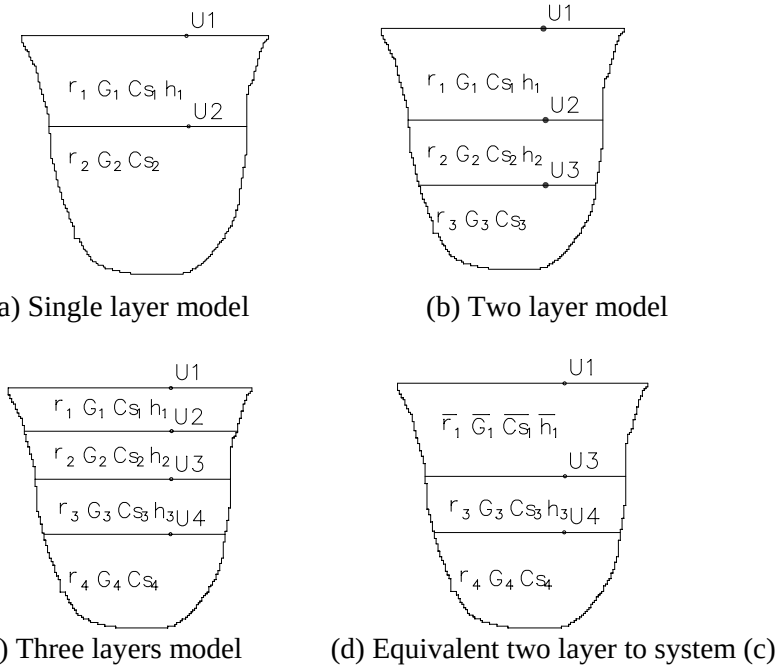

(a) Single layer model (b) Two layer model

(c) Three layers model (d) Equivalent two layer to system (c)

Figure 7. Idealized model for calculation of shear wave velocity

Table 3. Shear wave velocities for each layer identified

	EQ No.	1	2	3	4	5	6	7	8	9	10	11
	Layer	Cs (m/s)	Cs (m/s)	Cs (m/s)	Cs (m/s)	Cs (m/s)	Cs (m/s)	Cs (m/s)	Cs (m/s)	Cs (m/s)	Cs (m/s)	Cs (m/s)
EW	L1	195	221	206	185	201	199	235	182	155	143	181
	L2	263	246	241	240	219	248	310	245	198	241	249
	L3	296	329	323	302	321	315	372	441	221	302	315
	L4	426	448	527	573	348	530	516	436	316	371	333
NS	L1	224	245	235	225	193	208	247	199	180	188	216
	L2	394	361	357	356	307	355	433	426	324	353	368
	L3	451	556	549	403	408	449	514	407	350	349	394
	L4	533	606	645	610	583	577	672	647	478	561	596
	EQ No.	12	13	14	15	16	17	18	19	20	21	22
	Layer	Cs (m/s)	Cs (m/s)	Cs (m/s)	Cs (m/s)	Cs (m/s)	Cs (m/s)	Cs (m/s)	Cs (m/s)	Cs (m/s)	Cs (m/s)	Cs (m/s)
EW	L1	157	223	150	204	223	183	143	134	159	158	204
	L2	279	384	277	271	271	215	241	178	213	268	254
	L3	346	307	274	405	411	214	302	174	296	292	259
	L4	680	495	391	532	504	308	371	242	370	440	360
NS	L1	238	247	212	235	296	209	188	181	148	182	233
	L2	415	472	354	378	409	317	353	300	351	436	349
	L3	428	468	388	476	495	364	349	384	364	400	407
	L4	618	674	544	626	664	481	561	442	506	735	523

Shear wave velocities identified

Based on the procedure described above and the predominant frequencies shown in Table 2, the shear wave velocities for Layer L1(0~5.3m), Layer L2(5.3~15.8m), Layer L3(15.8~26.3m), and Layer L4(26.3~52.6m) can be calculated layer by layer. For all cases, the velocity profile identified from the NS and EW ground responses are summarized in Table 3. It shows that the velocities identified from the EW responses are smaller than those from the NS responses in general. It is as expected because the predominant frequencies obtained from spectral analyses have lower values in EW direction. Gunturi et al.(1998) had used the data of two earthquakes (Events 4 and 5 of this paper) to identify the shear wave velocities of soils by method of cross-correlation function, and similar results to this study were obtained except for the deepest layer.

Shear wave velocity vs. magnitude of ground shaking

To correlate the shear wave velocities with the magnitude of ground shaking, the shear wave velocities identified in Table 3 are plotted with respect to the PGA recorded at the depth of the top of each layer, as shown in Figures 8(a)~(d). It can be clearly seen that the shear wave velocity of each layer is decreased with the value of PGA recorded at the top of each layer, i.e., with the magnitude of ground shaking. This is due to the effect of nonlinearity of soil when it is subjected to larger shear strains. It can also be observed from those figures, the shear wave velocities identified have lower values in the EW direction as compared to the results in the NS direction. It is attributed from the effects of soil anisotropy. The same trend had been obtained from previous study (Hsu and Chen, 2003).

CONCLUSIONS

Based on the results obtained, some conclusions can be deduced as follows:

1. The method of phase spectrum identification is very effective to deduce the predominant frequency of vibration of soils by using the transfer function of earthquake responses recorded.
2. The predominant frequency of transfer function between the downhole earthquake response and the ground surface response will decrease with respect to the value of PGA at the ground surface. This is due to the effects of soil nonlinearity when the ground is subjected to larger excitations.
3. For the Hualien site, the shear wave velocity of each layer identified from the earthquake responses is decreased with respect to the value of PGA recorded at the top of each layer.
4. Both the predominant frequency of transfer functions calculated and the shear wave velocity of soil layers identified from earthquake responses show that the ground of Hualien site is anisotropic in two horizontal directions.

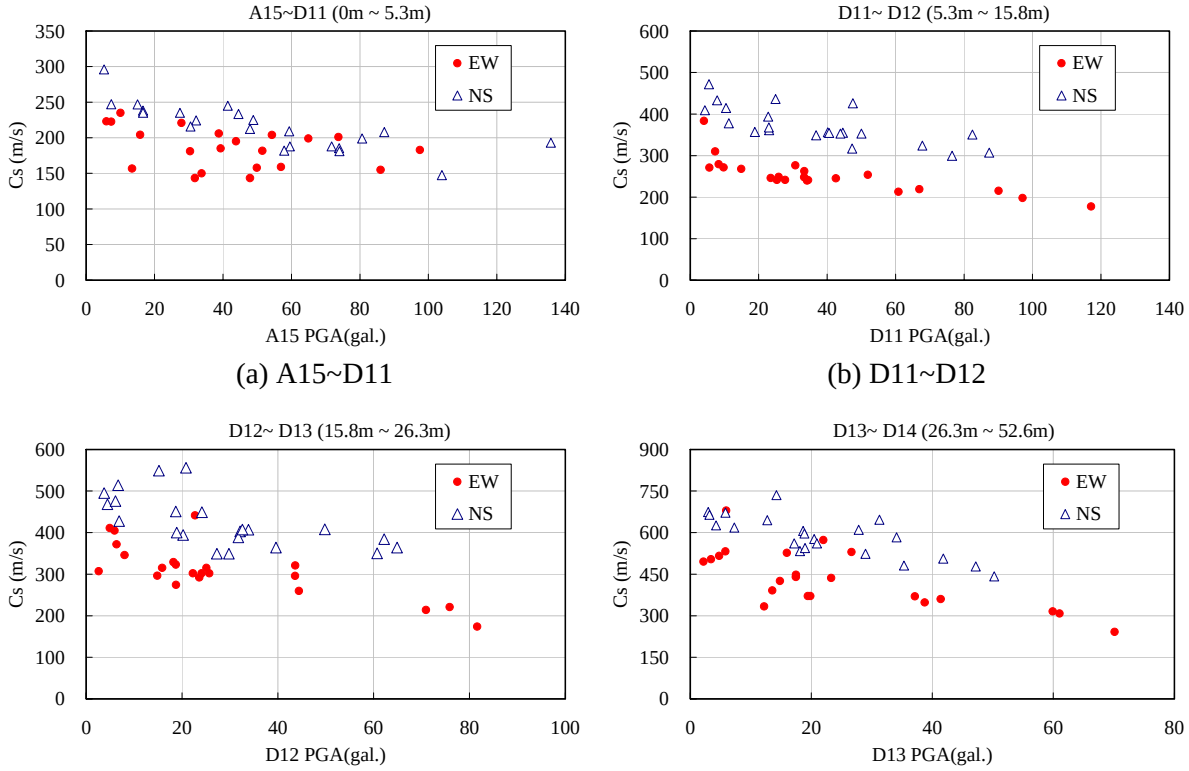

(a) A15~D11 (b) D11~D12

(c) D13~D14 (d) D14~D15

Figure 8. Shear wave velocity vs. PGA at the top of each layer

AKNOWLEDGEMENTS

Earthquake data provided by the Taipower company and financial support by the National Science Council of Taiwan (NSC – 90 - 2811 – E - 002 – 034) are deeply appreciated.

REFERENCES

Chen CH and Chiu HC. "Anisotropic seismic ground responses identified from the Hualien vertical array", Soil Dynamics and Earthquake Engineering, Vol 17, 371-395, 1998.

Chen CH and Chiu HC. "Identification of shear wave velocity from earthquake ground motions", Proc., 2nd Inter. Conf. Earthq. Geotech. Engrg., Lisbon, Portugal, 1:205-210, 1999.

Central Research institute of Electric Power industry (CRIEPI). "Soil Investigation Report for Hualien Project", Report, 1993.

de Barros, FCP and Luco JE. “Identification of foundation impedance functions and soil properties from vibration tests of the Hualien containment model”, Soil Dyn. Earthq. Engrg., 14:229-248, 1995.

Gunturi VR., Elgamal, AW and Tang HT. “Hualien seismic downhole data analysis”, Engrg. Geol.. 50(1-2):9-29, 1998.

Hsu SY and Chen CH. “Anisotropic Ground Response of the Hualien Containment Model,” Proc. of the Sixteenth KKCNN Symposium on Civil Engineering, Gyeongiu, Korea, 2003.

Pires JA and Higgins CJ. “Soil-structure interaction in cross-anisotropic site conditions”, Geotech. Special Pub., ASCE, Reston, Virginia, 2:1271-1282, 1998.

Seed HB and Idriss IM. “Shear Moduli and Damping Factors for Dynamic Response Analysis”, Report No. EERC-70/10, University of California, Berkeley, California, 1970.

Tang HT., et al. “The Hualien Large Scale Seismic Test for Soil-Structure Interaction Research”, Transactions of the 11th SMiRT, Tokyo, Japan, K04/4, 1991.

Tokyo Electric Power Co. (TEPCO). “Hualien LSST Project, Status Report of the forced Vibration Test Results, (Before Backfill) , (After Backfill) ”, Report, 1993.